

# Laser induced breakdown of the magnetic field reversal symmetry in the propagation of unpolarized light

G. S. Agarwal and Shubhrangshu Dasgupta

*Physical Research Laboratory, Navrangpura, Ahmedabad-380 009, India*

(November 21, 2018)

We show how a medium, under the influence of a coherent control field which is resonant or close to resonance to an appropriate atomic transition, can lead to very strong asymmetries in the propagation of unpolarized light when the direction of the magnetic field is reversed. We show how EIT can be used to mimic effects occurring in natural systems and that EIT can produce very large asymmetries as we use electric dipole allowed transitions. Using density matrix calculations we present results for the breakdown of the magnetic field reversal symmetry for two different atomic configurations.

PACS No(s):42.50.Gy,78.20.Ls,33.55.-b

## I. INTRODUCTION

It is well known how an isotropic medium becomes anisotropic by the application of a magnetic field [1]. In the special case when the magnetic field is parallel to the direction of the applied field and if we include the electric dipole contribution to susceptibilities, then the two circularly polarized light waves travel independently of each other. The propagation itself is determined by the magnetic field dependent optical susceptibilities  $\chi_{\pm}$ . If we write the incident field of frequency  $\omega$  in the form

$$\vec{E} \equiv (\mathcal{E}_+ \hat{e}_+ + \mathcal{E}_- \hat{e}_-) e^{ikz - i\omega t} + \text{c.c.}, \quad (1)$$

where

$$\hat{e}_{\pm} = \left( \frac{\hat{x} \pm i\hat{y}}{\sqrt{2}} \right), \quad \mathcal{E}_{\pm} = \left( \frac{\mathcal{E}_x \mp i\mathcal{E}_y}{\sqrt{2}} \right), \quad k = \frac{\omega}{c}, \quad (2)$$

the output field is given by

$$\vec{E}_0 = \vec{\mathcal{E}}_0 e^{ikz - i\omega t} + \text{c.c.}, \quad (3)$$

where

$$\vec{\mathcal{E}}_0 = \mathcal{E}_+ \hat{e}_+ e^{2\pi i k l \chi_+} + \mathcal{E}_- \hat{e}_- e^{2\pi i k l \chi_-}. \quad (4)$$

The susceptibilities  $\chi_{\pm}$  also depend on the frequency of the applied field. The rotation of the plane of polarization [2–7] and the dichroism can be calculated in terms of the real and imaginary parts of  $\chi_{\pm}$ . An interesting situation arises if the incident pulse is unpolarized. In that case there is a random phase difference between  $\mathcal{E}_x$  and  $\mathcal{E}_y$  and the intensities along two orthogonal directions are equal, i.e.,

$$\langle \mathcal{E}_x^* \mathcal{E}_x \rangle = \langle \mathcal{E}_y^* \mathcal{E}_y \rangle = \frac{I}{2}, \quad \langle \mathcal{E}_x^* \mathcal{E}_y \rangle = 0, \quad (5)$$

$I$  being the intensity of the incident pulse. From Eqs. (2)-(5), we can evaluate the output intensity  $I_0 = \langle |\vec{E}_0|^2 \rangle$ :

$$\begin{aligned} I_0 &\equiv \frac{I}{2} [|e^{2\pi i k l \chi_+}|^2 + |e^{2\pi i k l \chi_-}|^2] \\ &= \frac{I}{2} [\exp\{-4\pi k l \text{Im}(\chi_+)\} + \exp\{-4\pi k l \text{Im}(\chi_-)\}]. \end{aligned} \quad (6)$$

Thus the output intensity is a symmetric function of  $\chi_+$  and  $\chi_-$ . If the susceptibilities  $\chi_{\pm}$  obey the following relation when the direction of the magnetic field is reversed

$$\chi_{\pm}(B) = \chi_{\mp}(-B), \quad (7)$$

then

$$I_0(B) = I_0(-B). \quad (8)$$

Thus for unpolarized light the output intensity is the same whether the magnetic field is parallel or antiparallel to the direction of propagation of the electromagnetic field as long as (7) is satisfied.

In this paper we investigate if the transmission of unpolarised light through an otherwise isotropic medium can be sensitive to the direction of the magnetic field. We demonstrate how a suitably applied control field could make the transmission dependent on the direction of the magnetic field. This is perhaps the first demonstration of the dependence of transmission of the unpolarised light on the direction of  $B$ . For a large range of parameters we find that transmission could be changed by a factor of order two. We also report a parameter domain where the medium becomes opaque for one direction but becomes transparent for the reversed direction of the magnetic field. This work is motivated by the phenomena of optical activity and the magneto-chiral anisotropy which occur in many systems in nature [8–10]. The latter effect has recently become quite important. Several ingenious measurements of this effect have been made though the effect in natural systems is quite small. The smallness of the effect arises from the fact that the effect involves a combination of electric dipole, magnetic dipole and quadrupole effects[11–14]. The magnetochiral anisotropy is just the statement  $I(B)$  not equal to  $I(-B)$ . The effect we report is analogous but quite different in its physical content.

In this paper we show how rather large asymmetry between  $I_0(B)$  and  $I_0(-B)$  can be produced by using a coherent control field. The asymmetry could be large as we use only the electric dipole transitions. To demonstrate the idea we consider different specific situations depending on the transition on which the control field is applied. The control field can be used to modify, say,  $\chi_+$  leaving  $\chi_-$  unchanged [2,4,6,15]. Thus in presence of the control field we violate the equality (7) and this can result in large magneto-asymmetry in the propagation of unpolarized light. Such a large asymmetry, which we would refer to as magnetic field reversal asymmetry (BRAS in short), is induced by selectively applying the control field so as to break the time-reversal symmetry. It is important to note that we work with electric dipole transitions only. The control field is used to mimic the effects which occur in nature due to a combination of higher order multipole transitions.

The structure of our paper is as follows. In Sec. II, we will discuss how one can use a control field to create large BRAS. We present a very simple physical model. We present relevant analytical results. In Sec. III, we introduce another model, where the control field is applied such that we get a ladder system. We present the analytical results for BRAS in such a system. We also discuss the effect of atomic motion on BRAS in Sec. IV.

## II. LARGE MAGNETIC FIELD REVERSAL ASYMMETRY USING EIT

The application of a coherent pump leads to the well-studied electromagnetically induced transparency (EIT) [15] and coherent population trapping (CPT) [16]. The usage of pump and probe in a Lambda configuration is especially useful in suppressing the absorption of the probe, particularly if the lower levels of the  $\Lambda$  configuration are metastable and if the pump is applied between initially unoccupied levels. We explore how EIT can help in producing large BRAS. We first explain the basic idea in qualitative terms and then would produce detailed results using density matrix equations for several systems of interest.

Consider the following scenario. Let us consider first the case when  $\vec{B}$  is applied parallel to the direction of propagation of the electromagnetic field. Suppose the control field is applied such that the  $\sigma_+$  component becomes transparent, i.e.,  $\text{Im}[\chi_+(B)] \approx 0$ . For magnetic field bigger than the typical linewidth, the component  $\sigma_-$  is off-resonant. Thus  $\sigma_-$  exhibits very little absorption  $\text{Im}(\chi_-) \approx 0$ . Under such conditions, Eq. (6) shows that the transmitted intensity  $\approx I$ . Now if the direction of the magnetic field is reversed, then we easily find the situation when  $\sigma_+$  component becomes off resonant from the corresponding transition, i.e.,  $\text{Im}(\chi_+) \approx 0$ ; the  $\sigma_-$  component can become resonant and suffers large absorption, i.e., exhibits large  $\text{Im}(\chi_-)$ . This gives rise to an intensity

$\sim I/2$ . Thus the transmittivity reduces by a factor  $1/2$  upon reversal of the magnetic field. It is thus clear how coherent fields can be used to create large BRAS.

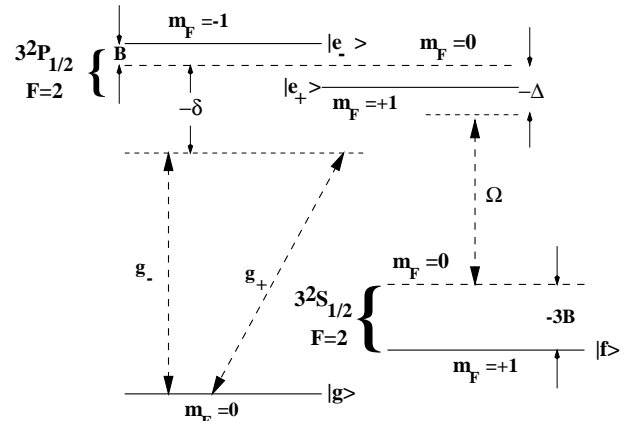


FIG. 1. The  $^{23}\text{Na}$  hyperfine level configuration is shown here. Here,  $B > 0$  is the applied magnetic field strength,  $2g_{\pm}$  are the probe Rabi frequencies for the  $\sigma_{\pm}$  components, and  $\Omega$  is the half of the pump Rabi frequency. The respective detunings  $\delta = [\omega_p - \omega_{e+g}(B = 0)]$  and  $\Delta$  for the probe and pump fields are defined with respect to the energy separation between the levels  $(|3^2P_{1/2}; F = 2, m_F = 0\rangle, |g\rangle)$  and  $(|3^2P_{1/2}; F = 2, m_F = 0\rangle, |3^2S_{1/2}; F = 2, m_F = 0\rangle)$ , respectively. Changing the direction of the magnetic field interchanges the positions of  $|e_- \rangle$  and  $|e_+ \rangle$ . Besides the level  $|f\rangle$  moves above the dashed line for  $|3^2S_{1/2}; F = 2, m_F = 0\rangle$ .

We now demonstrate the feasibility of these ideas. We consider a configuration [see Fig. 1] which can be found, for example, in hyperfine levels of  $^{23}\text{Na}$  [17]. The level  $|g\rangle$  ( $|3^2S_{1/2}; F = 1, m_F = 0\rangle$ ) is coupled to the upper level  $|e_- \rangle$  ( $|3^2P_{1/2}; F = 2, m_F = -1\rangle$ ) and  $|e_+ \rangle$  ( $|3^2P_{1/2}; F = 2, m_F = +1\rangle$ ) by the  $\sigma_-$  and  $\sigma_+$  components of the probe field. The susceptibilities for the two components of the probe acting on the transitions  $|g\rangle \leftrightarrow |e_- \rangle$  and  $|g\rangle \leftrightarrow |e_+ \rangle$  are given by

$$\chi_-(B) = \frac{-i\gamma\alpha_0}{i(\delta - B) - \Gamma_{e-g}}, \quad (9a)$$

$$\chi_+(B) = \frac{-i\gamma\alpha_0}{i(\delta + B) - \Gamma_{e+g}}, \quad \delta \equiv \omega - \omega_{e+g}(B = 0), \quad (9b)$$

where,  $\alpha_0$  is given by  $N|\vec{d}|^2/\hbar\gamma$  and is related to the absorption in the line-center for  $B = 0$ . It should be borne in mind that  $B$  represents the Zeeman splitting of the level  $m_F = -1$ . Thus  $B$  has the unit of frequency. Here  $2\gamma$  is the spontaneous decay rate from the level  $|e_- \rangle$ ,  $\Gamma_{e-g} = \gamma(\Gamma_{e+g} = 4\gamma/3)$  is the decay rate of the off-diagonal density matrix elements between level  $|e_- \rangle$  ( $|e_+ \rangle$ ) and  $|g\rangle$ ,  $N$  is the atomic number density,  $|\vec{d}|$  is the dipole moment matrix element between the levels  $|e_- \rangle$  and  $|g\rangle$ , and  $\delta$  is the detuning of the probe field from the  $|g\rangle \leftrightarrow |3^2P_{1/2}; F = 2, m_F = 0\rangle$  transition. Note that  $\delta$  would always be defined with respect to the levels in the absence of the magnetic field. Using the Eqs. (6) and (9),

one easily finds that the relation (8) holds for all  $\delta$ . In all equations,  $B$  would be considered as positive quantity.

To create a large asymmetry between the output intensities  $I_0(B)$  and  $I_0(-B)$ , we now apply a coherent control field

$$\vec{E}_p(z, t) = \vec{\mathcal{E}}_p(z) e^{-i\omega_p t} + \text{c.c.} \quad (10)$$

on the transition  $|e_+\rangle \leftrightarrow |f\rangle$  ( $|3^2S_{1/2}; F=2, m_F=+1\rangle$ ). This modifies the susceptibility  $\chi_+$  of the  $\sigma_+$  component to

$$\bar{\chi}_+(B) = \frac{-i\gamma\alpha_0[i(\delta - \Delta + 3B) - \Gamma_{fg}]}{[i(\delta + B) - \Gamma_{e+g}][i(\delta - \Delta + 3B) - \Gamma_{fg}] + |\Omega|^2}, \quad (11)$$

$$\Delta = \omega_p - \omega_{e+f}(B=0).$$

Here,  $\Delta = 2B$  is the detuning of the pump field from the transition  $|3^2P_{1/2}; F=2, m_F=0\rangle \leftrightarrow |3^2S_{1/2}; F=2, m_F=0\rangle$  transition [see Fig. 1],  $\Omega = \vec{d}_{e+f} \cdot \vec{\mathcal{E}}_p / \hbar$  is the half of the pump Rabi frequency. The parameter  $\Gamma_{fg}$  represents the collisional dephasing between the states  $|f\rangle$  and  $|g\rangle$ . In what follows we use  $\Gamma_{fg} = 0$ . The level  $|f\rangle$  is Zeeman separated from the level  $|3^2S_{1/2}; F=2, m_F=0\rangle$  by an amount of  $3B$ , whereas the levels  $|e_\pm\rangle$  are separated by an amount  $\mp B$ . These can be calculated from the Landé- $g$  factor of the corresponding levels. The susceptibility  $\bar{\chi}_-$  remains the same as in (9a). Note that in presence of the control field, the response of the system is equivalent to a two-level system comprised of ( $|e_-\rangle, |g\rangle$ ) [for  $\sigma_-$  component] and a  $\Lambda$ -system [for  $\sigma_+$  component] comprised of ( $|e_+\rangle, |f\rangle, |g\rangle$ ) connected via the common level  $|g\rangle$ .

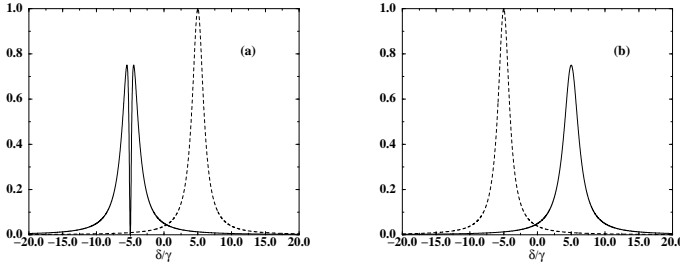


FIG. 2. The variation of imaginary parts of the susceptibilities  $\bar{\chi}_+$  (solid curve) and  $\bar{\chi}_-$  (dashed curve) in units of  $\alpha_0$  with probe detuning  $\delta/\gamma$  are shown for the  $\bar{\chi}_\pm(B)$  [(a)] and  $\bar{\chi}_\pm(-B)$  [(b)]. The parameters used here are  $\Omega = 0.5\gamma$ ,  $B = 5\gamma$  corresponding to 105 G,  $\Gamma_{e+g} = 4\gamma/3$ ,  $\Gamma_{fg} = 0$ ,  $\Gamma_{e-g} = \gamma$ , and  $\Delta = 2B$ .

It is clear that applying a coherent pump field, one can generate an EIT window at  $\delta = -B$  (cf.,  $\Delta = 2B$ ) for the  $\sigma_+$  component [ $\text{Im}(\bar{\chi}_+) = 0$ ]. On the other hand, the absorption peak of the  $\sigma_-$  component occurs at  $\delta = B$ . Thus, this component suffers a little absorption [ $\text{Im}(\bar{\chi}_-) \approx 0$ ] at  $\delta = -B$  as the field is far detuned from the  $|e_-\rangle \leftrightarrow |g\rangle$  transition as long as we choose the magnetic field much larger than the width of the transition [see Fig. 2(a)]. Thus the unpolarized probe field

travels through the medium almost unattenuated. The transmittivity  $T(B) = I_0(B)/I$  becomes almost unity at  $\delta = -B$  as obvious from Eq. (6) [see Fig. 3].

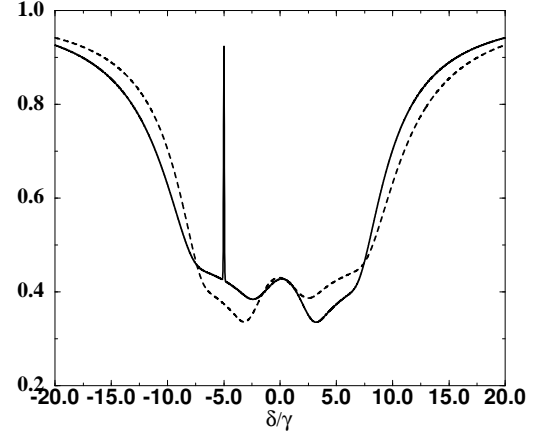


FIG. 3. This figure shows the variation of the transmittivity  $T(B)$  (solid curve) and  $T(-B)$  (dashed curve) with respect to probe field detuning  $\delta/\gamma$ . The parameters used here are  $N = 10^{10}$  atoms  $\text{cm}^{-3}$ ,  $\lambda = 589$  nm, and  $L = 1$  cm. All the other parameters used are the same as in Fig. 2.

If now the direction of the magnetic field is reversed ( $B \rightarrow -B$ ), then the corresponding susceptibilities for  $\sigma_-$  and  $\sigma_+$  polarizations become

$$\bar{\chi}_-(-B) = \frac{-i\gamma\alpha_0}{i(\delta + B) - \Gamma_{e-g}}, \quad (12a)$$

$$\bar{\chi}_+(-B) = \frac{-i\gamma\alpha_0[i(\delta - \Delta - 3B) - \Gamma_{fg}]}{[i(\delta - B) - \Gamma_{e+g}][i(\delta - \Delta - 3B) - \Gamma_{fg}] + |\Omega|^2}. \quad (12b)$$

We continue to take the quantization axis as defined by the direction of the propagation of the electromagnetic field. Clearly now at  $\delta = -B$ ,  $\bar{\chi}_-(-B)$  has absorption peak and  $\sigma_-$  component of the probe will be absorbed. If we continue to use  $\Delta = 2B$ , i.e., if we keep the control laser frequencies fixed while we change the direction of the magnetic field, then  $\bar{\chi}_+(-B)$  exhibits resonances at  $\delta = 3B \pm \sqrt{4B^2 + \Omega^2}$ , both of which are far away from the point  $\delta = -B$  unless we choose  $\Omega^2 = 12B^2$ . Clearly, for  $\delta = -B$  and  $\Omega^2 \neq 12B^2$ , the  $\sigma_+$  component of the probe will suffer very little absorption. This is in contrast to the behavior of the  $\sigma_-$  component which will be attenuated by the medium. Thus the output field would essentially have the contribution from the  $\sigma_+$  component. The transmittivity  $T(-B) = I_0(-B)/I$  of the medium decreases to about 1/2. Thus by using EIT we can produce the result  $T(B) \approx 2T(-B)$ , i.e., we can alter the transmittivity of the medium by just reversing direction of the magnetic field. The equality (8) no longer is valid and the medium behaves like a chiral medium. This becomes quite clear from the Fig. 3, at  $\delta = -B$ .

A quite a different result is obtained by choosing the parameter region differently. For the choice of the external field strength  $\Omega = 2\sqrt{3}B$ , and  $\Delta = 2B$ ,  $\delta = -B$ , the  $\sigma_+$  component gets absorbed significantly if the direction of the magnetic field is opposite to the direction of the propagation of the field. Thus  $T(-B)$  becomes insignificant compared to  $T(B)$  as shown in Fig. 4. For larger values of  $B$ , the result is shown in the inset. Here  $T(B)/T(-B)$  is in the range 2 to 3. Clearly, the case displayed in Fig. 4 is quite an unusual one. Such a large asymmetry in the dichroism of unpolarized light is the result of the application of a coherent control field whose parameters are chosen suitably.

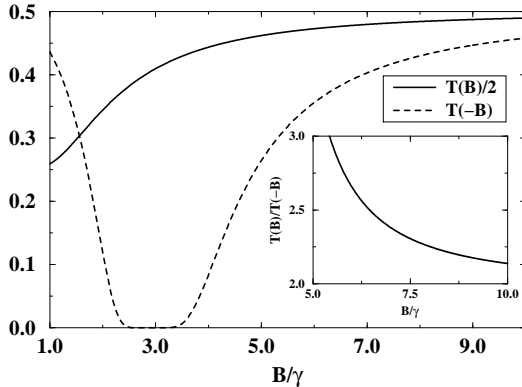


FIG. 4. The transmittivities  $T(B)$  and  $T(-B)$  calculated at the value  $\delta = -B$  is plotted here with respect to  $B/\gamma$ , for  $\Omega = 10\gamma$  and  $\Delta = 2B$ . The inset shows the magnetic field dependence of the ratio  $T(B)/T(-B)$  for the same parameters. All the other parameters are the same as in Fig. 3.

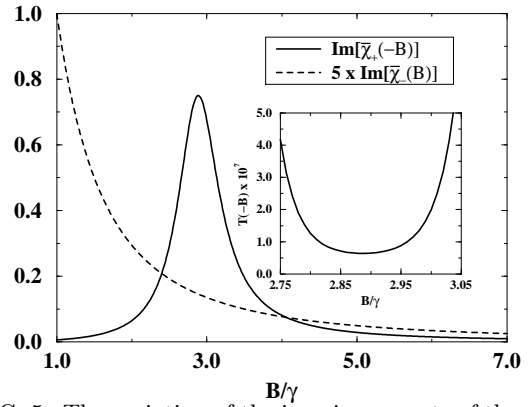


FIG. 5. The variation of the imaginary parts of the susceptibilities  $\chi_+(-B)$  and  $\chi_-(B)$  in units of  $\alpha_0$  with the magnetic field  $B/\gamma$  for  $\delta = -B$ . The inset shows the variation  $T(-B)$  with  $B$  in the vicinity of  $\Omega = 2\sqrt{3}B$ . The parameters used here are the same as in Fig. 4.

### III. LARGE MAGNETIC FIELD REVERSAL ASYMMETRY IN LADDER SYSTEM

The behavior shown in the Fig. 4 is easily understood from the magnitudes of the imaginary parts of the susceptibilities  $\chi_{\pm}(\pm B)$ . In the parameter domain under consideration,  $\text{Im}[\chi_+(B)] = 0$  (EIT);  $\text{Im}[\chi_-(-B)] = \alpha_0$ , because the  $\sigma_-$  component is on resonance for  $\vec{B}$  antiparallel to the direction of propagation. Further as shown in the Fig. 5, in the region around  $\Omega = 2\sqrt{3}B$ ,  $\text{Im}[\chi_-(B)] \ll \text{Im}[\chi_+(-B)]$ . Thus both  $\sigma_-$  and  $\sigma_+$  components are absorbed if  $\vec{B}$  is antiparallel  $\vec{k}$ , making the medium opaque as shown in the inset of Fig. 5. The opacity disappears if direction of  $\vec{B}$  is reversed (see Fig. 4, solid curve). For values of  $B$  away from the equality  $\Omega = 2\sqrt{3}B$ ,  $\text{Im}[\chi_+(-B)]$  decreases leading to an increase in the transmission  $T(-B)$ .

It may be recalled that there are many different situations where pump cannot be applied in a Lambda configuration. This, say, for example, is the case for  $^{40}\text{Ca}$ . The relevant level configuration is shown in Fig. 6 [4]. The level  $|g\rangle$  ( $|4s^2; j = 0, m_j = 0\rangle$ ) is coupled to  $|e_+\rangle$  ( $|4s4p; j = 1, m_j = +1\rangle$ ) and  $|e_-\rangle$  ( $|4s4p; j = 1, m_j = -1\rangle$ ) via the  $\sigma_+$  and  $\sigma_-$  components of the input unpolarized probe field, respectively. In this configuration, the susceptibilities of the two circularly polarized components of the probe are given by

$$\chi_+(B) = \frac{-i\gamma\alpha_0}{i(\delta - B) - \gamma}, \quad (13a)$$

$$\chi_-(B) = \frac{-i\gamma\alpha_0}{i(\delta + B) - \gamma}, \quad \delta = \omega - \omega_{e-g}(B = 0), \quad (13b)$$

where,  $\alpha_0 = N|\vec{d}|^2/\hbar\gamma$ ,  $N$  is the number density of the medium,  $\delta$  is the detuning of the probe field with respect to the  $|g\rangle \leftrightarrow |0\rangle$  ( $|4s4p; j = 1, m_j = 0\rangle$ ) transition,  $|\vec{d}|$  is the magnitude of the dipole moment matrix element between the levels  $|e_+\rangle$  and  $|g\rangle$ , and  $2\gamma$  is the decay rate from the levels  $|e_+\rangle$  and  $|e_-\rangle$  to the level  $|g\rangle$ . Note that the imaginary parts of the susceptibilities (13) are peaked at  $\delta = B$  and  $\delta = -B$ , respectively, and clearly predict perfect symmetry in the transmittivity of the medium upon reversal of the direction of the magnetic field.

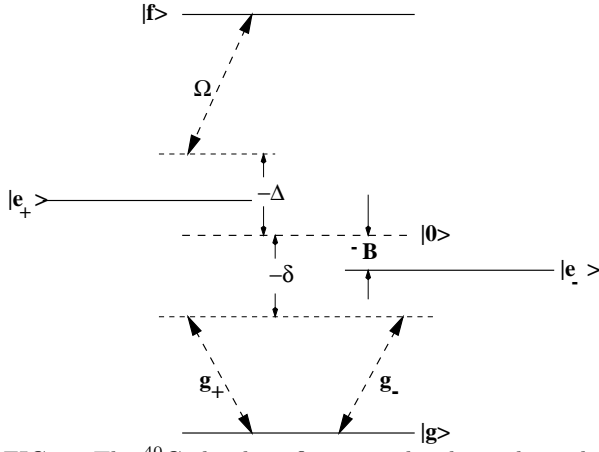


FIG. 6. The  $^{40}\text{Ca}$  level configuration has been shown here. Here,  $2g_{\pm}$  are the probe Rabi frequencies for the  $\sigma_{\pm}$  components,  $B$  is the magnetic field strength,  $\Omega$  is the half of the pump Rabi frequency,  $\delta$  and  $\Delta$  are the respective detuning for the probe and the pump fields. These detunings are defined with respect to the energy separation between the levels  $(|0\rangle, |g\rangle)$  and  $(|0\rangle, |f\rangle)$ , respectively.

We will now show how one can use a coherent control field to create asymmetry between  $T(B)$  and  $T(-B)$ . We apply a coherent pump (10) to couple  $|e_+\rangle$  with a higher excited level  $|f\rangle$  ( $|4p^2; j = 0, m_j = 0\rangle$ ) with Rabi frequency  $2\Omega = 2\vec{d}_{fe_+} \cdot \vec{\mathcal{E}}_p / \hbar$ . The susceptibility for  $\sigma_+$  component now changes to [2]

$$\bar{\chi}_+(B) = \frac{-i\gamma\alpha_0[i(\Delta + \delta) - \Gamma]}{[i(\delta - B) - \gamma][i(\Delta + \delta) - \Gamma] + |\Omega|^2},$$

$$\Delta = \omega_p - \omega_{fe_+} (B = 0), \quad (14)$$

where,  $\Gamma = 0.5(\lambda_{e+g}/\lambda_{fe_+})^3\gamma = 0.45\gamma$  is the spontaneous decay rate of the upper level  $|f\rangle$  [cf.,  $\lambda_{e+g} = 422.7$  nm and  $\lambda_{fe_+} = 551.3$  nm],  $\lambda_{\alpha\beta}$  is the wavelength of the transition between  $|\alpha\rangle$  and  $|\beta\rangle$ ,  $\Delta = -B$  is the detuning of the pump field from the  $|f\rangle \leftrightarrow |0\rangle$  transition [see Fig. 6]. Thus a transparency dip in the absorption profile of the  $\sigma_+$  component at  $\delta = B$  is generated and the  $\sigma_-$  component remains far-detuned from the corresponding transition, as shown in Fig. 7(a). Note that the transparency for  $\sigma_+$  is not total which is in contrast to a Lambda system. We display in the Fig. 8 the behavior of the transmittivity  $T(B)$  of the medium as a function of the detuning.

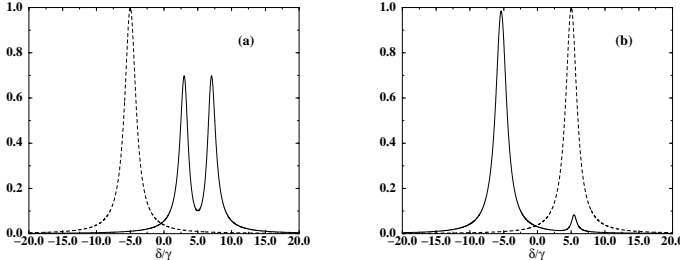


FIG. 7. The variation of imaginary parts of the susceptibilities  $\bar{\chi}_+$  (solid curve) and  $\bar{\chi}_-$  (dashed curve) in units of  $\alpha_0$  with respect to the probe detuning  $\delta/\gamma$  are shown here for  $\bar{\chi}_{\pm}(B)$  [(a)] and  $\bar{\chi}_{\pm}(-B)$  [(b)]. The parameters used here are  $\Omega = 0.5\gamma$ ,  $B = 5\gamma$  corresponding to 123 G,  $\Gamma = 0.45\gamma$ , and  $\Delta = -B$ .

Now upon reversal of the magnetic field direction, the  $\sigma_+$  component gets detuned from corresponding transition and thereby suffers little absorption. The  $\sigma_-$  component, being resonant with the corresponding transition, gets largely attenuated inside the medium. This is clear from the Fig. 7(b). Thus the contribution to the transmittivity  $T(-B)$  comes primarily from the  $\sigma_+$  component. The Fig. 8 exhibits the behavior of  $T(-B)$  as the frequency of the probe is changed. In the region of EIT,  $T(B)$  is several times of  $T(-B)$ .

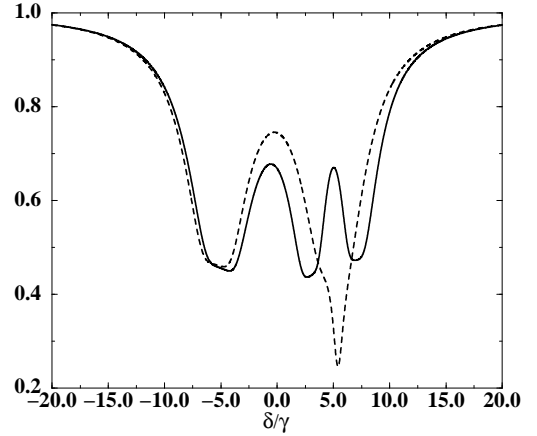


FIG. 8. The variation for the transmittivities  $T(B)$  (solid curve) and  $T(-B)$  (dashed curve) with the probe detuning  $\delta/\gamma$  are shown in this figure. The parameters used here are  $N = 10^{10}$  atoms  $\text{cm}^{-3}$ ,  $\lambda_{e+g} = 422.7$  nm,  $L = 1$  cm, and the other parameters are the same as in Fig. 7.

In Fig. 9, we have shown how the ratio  $T(B)/T(-B)$  calculated at  $\delta = B$  is modified with change in the magnitude of the applied magnetic field for different control field Rabi frequencies. Note that for large  $B$  and  $\Omega$ , this ratio approaches the value of two, though for intermediate values it can exceed two.

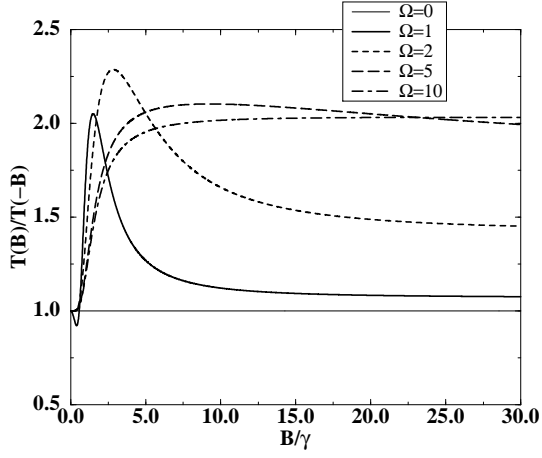


FIG. 9. The variation of the ratio  $T(B)/T(-B)$  calculated at  $\delta = B$  with the magnetic field strengths  $B/\gamma$  are shown in this figure for different values of  $\Omega$ . All the parameters are the same as in Fig. 8.

#### IV. MAGNETIC FIELD REVERSAL ASYMMETRY IN THE PROPAGATION OF AN UNPOLARIZED BEAM THROUGH A DOPPLER BROADENED MEDIUM

We next consider the effects of Doppler broadening on the BRAS in a Lambda configuration. We would like to find parameter regions where  $T(B)$  and  $T(-B)$  could differ significantly. We identify the spatial dependence of the pump  $\mathcal{E}_p(z) = e^{ik_p z}$  and  $\Delta_v = 2B + k_p v_z$ , where  $v_z$  is the component of the atomic velocity in the direction of the propagation of the electric fields. We assume that the pump field propagates in the same direction  $\vec{k}_p$  as the probe field wave vector  $\vec{k}$  and we further take  $k$  and  $k_p$  to be approximately equal.

We calculate the Doppler-averaged susceptibilities through the following relation:

$$\langle \bar{\chi}_{\pm}(v_z) \rangle = \int_{-\infty}^{\infty} \bar{\chi}_{\pm}(v_z) \sigma_D(v_z) dv_z, \quad (15)$$

where,

$$\sigma_D(v_z) = \frac{1}{\sqrt{2\pi\omega_D^2}} e^{-v_z^2/2\omega_D^2} \quad (16)$$

is the Maxwell-Boltzmann velocity distribution at a temperature  $T$  with the width  $\omega_D = \sqrt{K_B T/M}$ ,  $K_B$  is the Boltzmann constant, and  $M$  is the mass of an atom.

The integration (15) results in a complex error function [18]. However, to have a physical understanding, we integrate (15) by approximating  $\sigma_D$  by a Lorentzian  $\sigma_L(v_z)$  of the width  $\tilde{\omega}_D = 2\omega_D \ln 2$  [19]:

$$\sigma_L(v_z) = \frac{\tilde{\omega}_D/\pi}{v_z^2 + \tilde{\omega}_D^2}. \quad (17)$$

This leads to the following approximate results:

$$\langle \bar{\chi}_{\pm}(v_z) \rangle = \frac{\gamma \alpha_0}{k(v_{\pm} - i\tilde{\omega}_D)}, \quad (18)$$

where,

$$\begin{aligned} v_+ &= \frac{i\{[i(\delta + B) - \Gamma_{e+g}]P + |\Omega|^2\}}{kP}, \\ P &= i(\delta - \Delta + 3B) - \Gamma_{fg}, \\ v_- &= \frac{i[i(\delta - B) - \Gamma_{e-g}]}{k}. \end{aligned} \quad (19)$$

Here we have used the expressions (9a) and (11) for  $\bar{\chi}_{\pm}(v_z)$ . These susceptibilities (18) are used to calculate the transmittivities at the point  $\delta = -B$ . In Fig. 10 we have shown the corresponding variation of  $T(B)$  and  $T(-B)$  with  $\delta/\gamma$ . We find that the ratio  $T(B)/T(-B)$  increases to a value  $\sim 1.6$ , for a 6 cm medium.

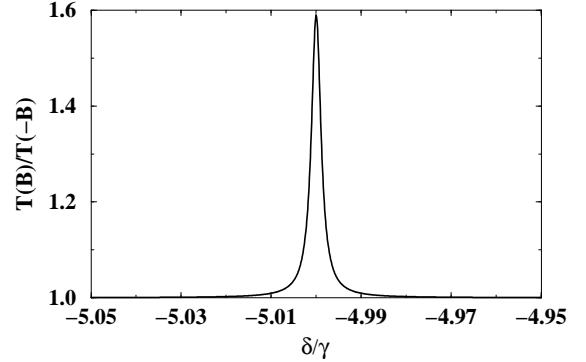


FIG. 10. The variation in  $T(B)/T(-B)$  with the probe detuning  $\delta/\gamma$  in a 6 cm Doppler-broadened medium. All the other parameters are the same as in Fig. 4. Note that  $T(B)$  is the transmission for  $\vec{B}$  parallel to  $\vec{k}$ .

It is clear that, if we choose a longer medium in this case, the BRAS will be further enhanced. We have actually also carried out numerically the integration (15). For the parameters of the Fig. 10, the results do not change substantially.

#### V. CONCLUSIONS

In conclusion, we have shown how one can make use of a coherent field to create large BRAS in the propagation of an unpolarized light. We have discussed two different system configurations. We have shown how EIT can be used very successfully to produce large BRAS. We have also analyzed the effect of Doppler broadening and found the interesting region of parameters with large asymmetry.

- [1] L. D. Landau, E. M. Lifshitz, and L. P. Pitaevski, *Electrodynamics of Continuous Media* (Pergamon, Oxford, 1984).
- [2] A. K. Patnaik and G. S. Agarwal, *Opt. Commun.* **179**, 97 (2000).
- [3] M. O. Scully and M. Fleischhauer, *Phys. Rev. Lett.* **69**, 1360 (1992); M. Fleischhauer and M. O. Scully, *Phys. Rev. A* **49**, 1973 (1994); M. Fleischhauer, A. B. Matsko, and M. O. Scully, *ibid.* **62**, 013808 (2000).
- [4] S. Wielandy and A. L. Gaeta, *Phys. Rev. Lett.* **81**, 3359 (1998).
- [5] B. Stahlberg, P. Jungner, T. Fellman, K.-A. Suominen, and S. Stenholm, *Opt. Commun.* **77**, 147 (1990); K.-A. Suominen, S. Stenholm, and B. Stahlberg, *J. Opt. Soc. Am. B* **8**, 1899 (1991).
- [6] A. K. Patnaik and G. S. Agarwal, *Opt. Commun.* **199**, 109 (2001); V. A. Sautenkov, M. D. Lukin, C. J. Bednar, I. Novikova, E. Mikhailov, M. Fleischhauer, V. L. Velichansky, G. R. Welch, and M. O. Scully, *Phys. Rev. A* **62**, 023810 (2000).
- [7] D. Budker, V. Yashchuk, and M. Zolotarev, *Phys. Rev. Lett.* **81**, 5788 (1998); D. Budker, D. F. Kimball, S. M. Rochester, V. V. Yashchuk, and M. Zolotarev, *Phys. Rev. A* **62**, 043403 (2000).
- [8] G. L. J. A. Rikken and E. Raupach, *Phys. Rev. E* **58**, 5081 (1998).
- [9] G. L. J. A. Rikken and E. Raupach, *Nature (London)* **390**, 493 (1997).
- [10] M. Vallet, R. Ghosh, A. Le Floch, T. Ruchon, F. Bretenaker, and J.-Y. Thépôt, *Phys. Rev. Lett.* **87**, 183003 (2001).
- [11] G. Wagnière and A. Meier, *Chem. Phys. Lett.* **93**, 78 (1982).
- [12] L. D. Barron and J. Vrbancich, *Mol. Phys.* **51**, 715 (1984).
- [13] N. B. Baranova and B. Ya. Zel'dovich, *Mol. Phys.* **38**, 1085 (1979).
- [14] L. D. Barron, *Nature (London)* **405**, 895 (2000).
- [15] S. E. Harris, *Phys. Today* **50** (7), 46 (1997).
- [16] E. Arimondo, *Progress in Optics XXXV*, Edited by E. Wolf (Elsevier, New York, 1996), p. 257.
- [17] I. Carusotto, M. Artoni, G. C. La Rocca, and F. Bassani, *Phys. Rev. Lett.* **87**, 064801 (2001).
- [18] M. Abramowitz and I. A. Stegun, *Handbook of Mathematical Functions*, (Dover Publication, New York, 1972).
- [19] M. M. Kash, V. A. Sautenkov, A. S. Zibrov, L. Hollberg, G. R. Welch, M. D. Lukin, T. Rostovtsev, E. S. Fry, and M. O. Scully, *Phys. Rev. Lett.* **82**, 5229 (1999).